An ELISA method to assess HDAC inhibitor-induced alterations to *P. falciparum* histone lysine acetylation

Eva Hesping [a], Tina S. Skinner-Adams [a], Gillian M. Fisher [a], Thomas Kurz [b], Katherine T. Andrews [a,*]

[a] *Griffith Institute for Drug Discovery, Griffith University, Brisbane, Australia*
[b] *Institut für Pharmazeutische und Medizinische Chemie, Heinrich Heine Universität, Düsseldorf, Germany*

ARTICLE INFO

ABSTRACT

The prevention and treatment of malaria requires a multi-pronged approach, including the development of drugs that have novel modes of action. Histone deacetylases (HDACs), enzymes involved in post-translational protein modification, are potential new drug targets for malaria. However, the lack of recombinant *P. falciparum* HDACs and suitable activity assays, has made the investigation of compounds designed to target these enzymes challenging. Current approaches are indirect and include assessing total deacetylase activity and protein hyperacetylation via Western blot. These approaches either do not allow differential compound effects to be determined or suffer from low throughput. Here we investigated dot blot and ELISA methods as new, higher throughput assays to detect histone lysine acetylation changes in *P. falciparum* parasites. As the ELISA method was found to be superior to the dot blot assay using the control HDAC inhibitor vorinostat, it was used to evaluate the histone H3 and H4 lysine acetylation changes mediated by a panel of six HDAC inhibitors that were shown to inhibit *P. falciparum* deacetylase activity. Vorinostat, panobinostat, trichostatin A, romidepsin and entinostat all caused an ~3-fold increase in histone H4 acetylation using a tetra-acetyl lysine antibody. Tubastatin A, the only human HDAC6-specific inhibitor tested, also caused H4 hyperacetylation, but to a lesser extent than the other compounds. Further investigation revealed that all compounds, except tubastatin A, caused hyperacetylation of the individual N-terminal H4 lysines 5, 8, 12 and 16. These data indicate that tubastatin A impacts *P. falciparum* H4 acetylation differently to the other HDAC inhibitors tested. In contrast, all compounds caused hyperacetylation of histone H3. In summary, the ELISA developed in this study provides a higher throughput approach to assessing differential effects of antiplasmodial compounds on histone acetylation levels and is therefore a useful new tool in the investigation of HDAC inhibitors for malaria.

1. Introduction

Almost half the world's population is at risk of infection with malaria parasites and despite recent gains in disease control, malaria remains a significant cause of global mortality and morbidity. In 2018, there were >200 million cases of malaria and an estimated 405,000 malaria associated deaths worldwide, mainly due to infection with *P. falciparum* (World Health Organisation 2019). While drugs remain the mainstay treatment strategy, increasing rates of drug resistance are a major concern, including resistance to current gold-standard artemisinin-based combination therapies (ACTs) (Chenet et al., 2016; Lu et al., 2017; Rasmussen et al., 2017; van der Pluijm et al., 2019; Uwimana et al., 2020). This is a significant problem which compromises malaria

elimination and eradication efforts (World Health Organisation 2019) and is driving the need to discover and develop new antimalarial agents with novel modes of action.

In *P. falciparum* a number of epigenetic regulatory proteins are under investigation as possible new antiplasmodial drug targets, including histone deacetylases (HDACs) (Andrews et al., 2012b; Andrews et al., 2012c; Fioravanti et al., 2020). HDACs, together with histone acetyltransferases (HATs), mediate the reversible acetylation of histone and non-histone proteins in eukaryotic cells and by doing so, regulate gene expression and other important cellular processes (Shahbazian and Grunstein 2007; Khan and La Thangue 2012; Hollin et al., 2020). *P. falciparum* has five annotated HDACs and one putative HDAC pseudogene (PlasmodDB gene ID: PF3D7_0506600) (Andrews et al., 2012a;

Andrews et al., 2012c; Kanyal et al., 2017). *Pf*HDAC1 (PlasmoDB gene ID: PF3D7_0925700) has the highest homology to human zinc-dependent class I HDACs (Andrews et al., 2008; Melesina et al., 2015; Hailu et al., 2017) while *Pf*HDAC2 (*Pf*HDA1; PlasmoDB gene ID: PF3D7_1472200) and *Pf*HDAC3 (*Pf*HDA2; PlasmoDB gene ID: PF3D7_1008000) are homologous to zinc-dependent class II HDACs (Kanyal et al., 2017). *Pf*Sir2A (PlasmoDB gene ID: PF3D7_1328800) and *Pf*Sir2B (PlasmoDB gene ID: PF3D7_1451400) are NAD^+-dependent enzymes and show highest homology to class III HDACs (Duraisingh et al., 2005; Freitas-Junior et al., 2005; Tonkin et al., 2009). *Pf*HDAC1, *Pf*HDAC2 and *Pf*HDAC3 are essential to the parasite, whereas the *Pf*HDAC pseudogene and *Pf*Sir2A and *Pf*Sir2B, which play a role in virulence, are not essential to asexual intraerythrocytic *P. falciparum* parasites (Aurrecoechea et al., 2009; Coleman et al., 2014; Zhang et al., 2018; Duraisingh et al., 2005; Merrick and Duraisingh 2007; Tonkin et al., 2009).

HDACs are well validated drug targets for cancer and to date, four HDAC inhibitors have been approved by the FDA for clinical use: vorinostat (Grant et al., 2007), panobinostat (Garnock-Jones 2015), romidepsin (Prince et al., 2013) and belinostat (Thompson 2014). The positive outcome of HDAC inhibitor treatment in cancer patients has triggered the investigation of HDAC inhibitors for other diseases including malaria. Since the first report of antiplasmodial activity of the cyclic tetrapeptide HDAC inhibitor apicidin in 1996 (Darkin-Rattray et al., 1996), HDAC inhibitors of different structural classes have been investigated for *in vitro* activity against malaria parasites (e.g. (Andrews et al., 2009; Andrews et al., 2012b; Andrews et al., 2012c; Fioravanti et al., 2020)). HDAC inhibitors with a hydroxamic acid zinc binding group have generally demonstrated the highest potency against *P. falciparum in vitro,* with varying levels of selectivity for the parasite versus human cells (Andrews et al., 2009; Andrews et al., 2012c; Giannini et al., 2015; Coetzee et al., 2020; Fioravanti et al., 2020). However, the lack of recombinant *P. falciparum* HDAC enzymes (*Pf*HDAC1 is commercially available but has low purity (Ontoria et al., 2016)) and crystal structures (none available) remains a major limitation to the rational design of new compounds with improved potency and parasite-specific selectivity. As a result, indirect approaches are used to investigate HDAC inhibitor activity and their effect on *Plasmodium* acetylation. This includes assessing the inhibition of deacetylase activity in *P. falciparum* protein lysates (e.g. (Agbor-Enoh et al., 2009; Engel et al., 2015)) and the detection of protein hyperacetylation via Western blot (e.g. (Sumanadasa et al., 2012; Engel et al., 2015)). Deacetylase inhibition assays do not provide any information about isotype specificity or allow differentiation of the effects of different compounds beyond inhibition levels. While Western blot analysis can provide information on differential effects of compounds in altering acetylation of different histone or non-histone lysine residues (Engel et al., 2015), this approach suffers from low throughput. In this study, two higher throughput methods (dot blot and enzyme-linked immunosorbent assay (ELISA)) were investigated to assess histone H4 lysine acetylation alterations following exposure of asexual-stage *P. falciparum* parasites to the HDAC inhibitor vorinostat. Of the two methods, ELISA was found to be more reproducible and sensitive than dot blot. To assess the ability of the ELISA method to discern differential changes in acetylation profiles within *P. falciparum* parasites, a panel of clinically approved and experimental anti-cancer HDAC inhibitors with differing human HDAC selectivity profiles was assessed using histone H3 and H4 specific antibodies.

2. Material and methods

2.1. Compounds

Vorinostat and chloroquine diphosphate salt were sourced from Sigma-Aldrich (USA). Entinostat (MS-275) and panobinostat (LBH589) were purchased from Selleck Chemicals (USA), romidepsin (FK228) from AdooQ Bioscience (USA), tubastatin A from Compounds Australia

(Original source: Selleck Chemicals, USA) and trichostatin A from Merck Millipore (USA). Stock solutions were prepared in 100% DMSO and stored at −20 °C.

2.2. P. falciparum in vitro culture and growth inhibition assays

P. falciparum 3D7 (Walliker et al., 1987) parasites were cultured *in vitro* in 5% O rhesus (Rh) positive human erythrocytes in sterile RPMI 1640 media (Gibco, USA) supplemented with 10% heat inactivated human sera and 5 μg/mL gentamycin (Sigma Aldrich, USA), as previously described (Trager and Jensen 2005; Andrews et al., 2008). Parasite cultures were incubated at 37 °C in 5% O_2 and 5% CO_2 in N_2 (BOC Gas, Australia) and synchronised using sorbitol treatment (Lambros and Vanderberg 1979). *In vitro* asexual *P. falciparum* 3D7 growth inhibition assays were carried out as previously described (Andrews et al., 2008). Briefly, synchronous ring-stage infected erythrocytes (0.5% parasitemia and 2.5% hematocrit) were cultured in triplicate wells with test compounds or controls (chloroquine and vorinostat). DMSO vehicle was used as negative control (<0.5% DMSO) and the concentration was constant in all wells of an individual assay. Following incubation at 37 °C for 48 h, $[^3H]$-hypoxanthine (0.5 μCi/well) was added and after a further 24 h incubation, cells were harvested onto MicroBeta 1450 filter mats (Wallac). $[^3H]$-hypoxanthine incorporation was determined using a MicroBeta 1450 liquid scintillation counter and the 50% inhibitory concentrations (IC_{50}s) were calculated and expressed as the average, plus and minus standard deviation (±SD), of three independent experiments performed in triplicate.

2.3. HDAC inhibitor treatment and protein lysate preparation

Protein hyperacetylation assays were carried out as previously published (Sumanadasa et al., 2012). Briefly, synchronised trophozoite-stage *P. falciparum* 3D7 parasites (3–5% parasitemia, 5% hematocrit) were incubated in 6-well plates with 5x IC_{50} of test compounds or controls (vorinostat as positive HDAC inhibitor control; chloroquine as non-HDAC inhibitor control) and DMSO as vehicle control for 3 h. Cells were harvested via centrifugation (1900 rpm, 2 min) and stored at −20 °C until use. Cells were thawed on ice, lysed using 0.15% saponin in phosphate-buffered saline buffer (PBS), pelleted via centrifugation and parasite pellets washed three times with PBS. Protein for Western blot analysis was prepared as previously described (Engel et al., 2015). For dot blot and ELISA, parasite pellets were resuspended in 250–500 μL PBS, depending on the sample size, and lysed via sonication (Branson Ultrasonics Corporation, USA; 2 × 2 min on ice in-between cycles, duty cycle: 20%, output control: 2, frequency: 20 kHz). Protein lysate concentrations were determined via Bradford Assay (Protein Assay Kit II, BioRad, #5000002, USA) and samples stored at −20 °C.

2.4. Dot blot

Dot blots were carried out using a Bio-Dot® microfiltration apparatus (Biorad, USA). Polyvinylidene fluoride membrane (PVDF, Immobilon®-FL; Merck, Germany) was activated with methanol, as per manufacturer's instructions, and placed into the Bio-Dot® microfiltration apparatus. After pre-hydration of membranes with three washes of 200 μL/well 1x transfer buffer (0.30% w/v Tris (AppliChem, Germany), 1.44% w/v Glycine (Chem-Supply, Australia), 20% Methanol (Chem-Supply, Australia)) using vacuum filtration, the protein lysate samples (100 μL per well; diluted with PBS) were added at concentrations ranging from 2 to 20 μg/mL and allowed to passively filter through the membranes. Membranes were washed three times with PBS (200 μL per well) via vacuum filtration and removed from the apparatus. After assessing protein load per sample using REVERT Protein Stain® (Li-Cor Biosciences, USA), membranes were blocked with Odyssey blocking buffer (Li-Cor Biosciences, USA; 1 h at room temperature) and
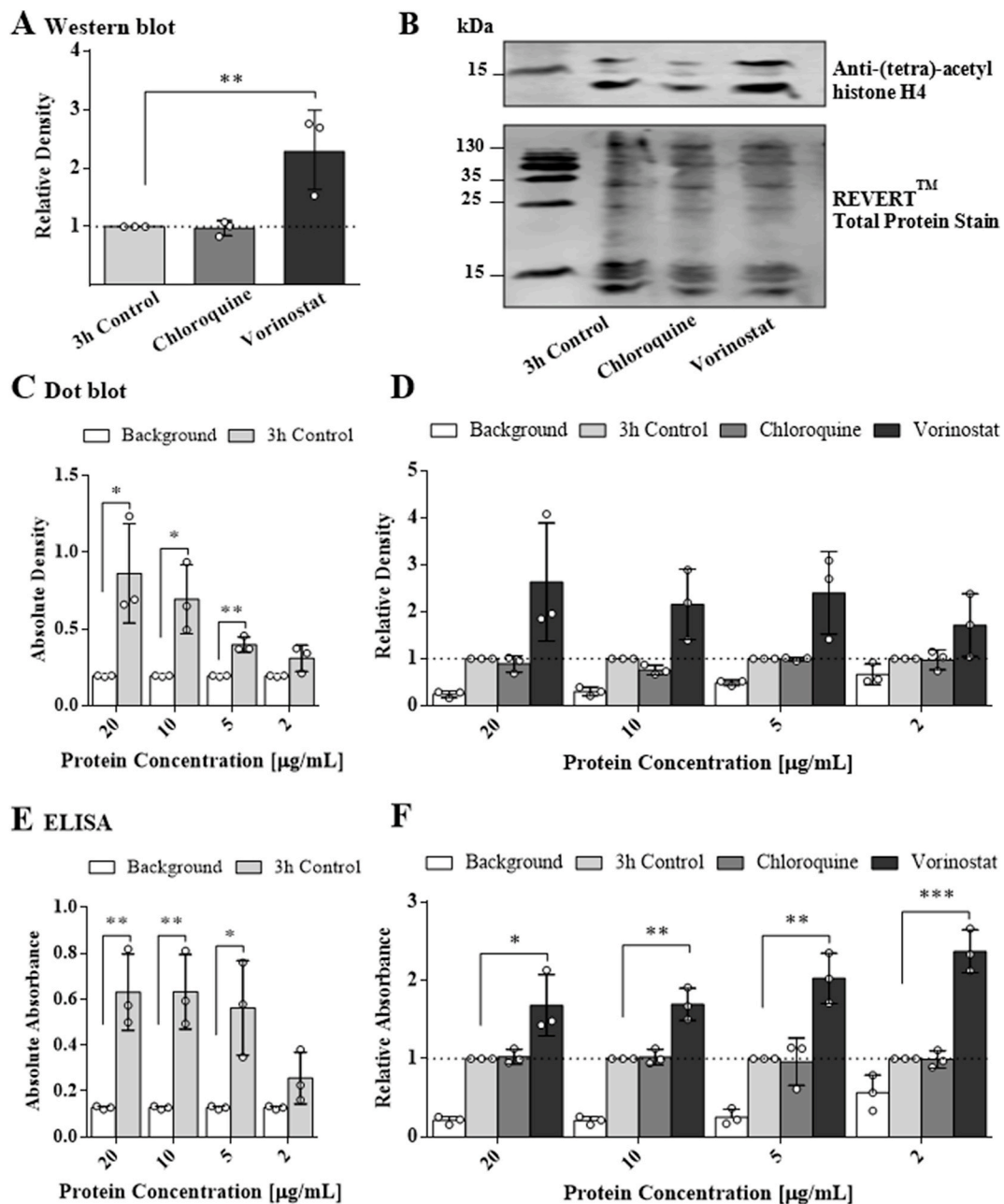
Fig. 1. Comparison of Western blot, dot blot and ELISA H4 acetylation detection in *P. falciparum* protein lysates. Western blot (**A** and **B**), dot blot (**C** and **D**) and ELISA (**E** and **F**) analysis of protein lysates prepared from trophozoite-stage *P. falciparum* 3D7 infected erythrocytes treated for 3 h with 5x IC$_{50}$ chloroquine or vorinostat and untreated DMSO vehicle control (3 h Control, 0.125% DMSO). Western blots and dot blots were carried out using anti-(tetra)-acetyl histone H4 primary antibody (1:2000 diluted in Odyssey blocking buffer) and goat anti-rabbit IRDye 680 as secondary antibody (1:10,000 diluted in Odyssey blocking buffer). Total protein was detected using REVERT™ total protein stain on the same membrane. Density signals were normalised to total protein load in the respective lane or dot blot well (absolute signal), then normalised (relative signal) to the untreated control (3 h Control) and expressed as fold change (3 h Control taken as 1.0; dotted line). ELISA was carried out using anti-(tetra)-acetyl histone H4 primary antibody (1:4000 diluted in 5% BSA in PBS) and goat anti-rabbit IgG (H/L): horseradish peroxidase (HRP) conjugate secondary antibody (1:2000 in PBS). Absorbance signals were read at 450 nm (absolute signal) and normalised (relative signal) to the untreated control (3 h Control) and expressed as fold change (3 h Control taken as 1.0; dotted line). For Western blot, one representative blot is shown (**B**). Graphs show mean absolute or relative density signals of Western blot (**A**) and dot blot (**C** and **D**) or ELISA absorbance signals (**E** and **F**)) for three independent biological samples (±SD). *P* values * <0.05, ** <0.01, *** <0.001; multiple student's t-tests. Data from individual experiments shown in Supplementary Information **S1**.

immunoblotted with anti-(tetra)-acetyl histone H4 (1:2000 dilution; Merck Millipore, USA, #06–866, diluted in Odyssey blocking buffer) at 4 °C overnight. Membranes were then washed three times with PBS for 10 min each wash, prior to adding IRDye 680 goat anti-rabbit secondary antibody (1:10,000; Li-Cor Biosciences, USA, #926–68071 diluted in Odyssey blocking buffer) and incubation at room temperature for 45 min. After three washing steps with PBS, membranes were imaged using the Odyssey Fc Dual-Mode Imaging System (Li-Cor Biosciences, USA) and densitometry analysis carried out using Image Studio Lite 5.2. Dot blot signal densities were normalised to total protein and expressed as fold change compared to the DMSO vehicle control (3 h Control; set to one). Data are presented as mean ± SD and the significant difference between the 3 h control and test compounds was analysed using a Student's t-test.

2.5. Enzyme-linked immunosorbent assay (ELISA)

Protein lysates (39 ng/mL – 20 μg/mL in PBS; 100 μL/well) were incubated in 96 well polystyrene plates (Greiner Bio-One, Austria) for 90 min at room temperature. Protein was aspirated and each well washed three times with PBS (200 μL/well), followed by blocking with 5% bovine serum albumin (BSA) in PBS for 1 h at room temperature. Primary antibodies (anti-(tetra)-acetyl histone H4 (1:4000 dilution; Merck Millipore, USA, #06–866), anti-acetyl histone H3 (1:2000 dilution; Merck Millipore, USA, #06–559), anti-acetyl histone H4 Lysine 5 (1:2000 dilution; Merck Millipore, USA, #07–327), anti-acetyl histone H4 Lysine 8 (1:2000 dilution; Merck Millipore, USA, #07–328), anti-acetyl histone H4 Lysine 12 (1:2000 dilution; Merck Millipore, USA, #07–595), anti-acetyl histone H4 Lysine 16 (1:1000 dilution; Merck Millipore, USA, #07–329)) were incubated for 1 h at room temperature (100 μL/well; diluted in PBS with 5% BSA). After aspirating primary antibodies, the wells were washed with PBS three times (200 μL per well), and secondary antibody added (1:2000 goat anti-rabbit IgG (H + L)-horseradish peroxidase (HRP) conjugate, Bio-Rad, USA, #1706515, 100 μL/well; diluted in PBS) followed by incubation for 1 h at room temperature. Wells were washed three times with PBS (200 μL/well) and 100 μL/well substrate solution added (0.1 mg/mL tetramethylbenzidine (TMB), 0.1% hydrogen peroxide (30% w/w), 200 mM disodium hydrogen phosphate, 100 mM citric acid, pH 4) and incubated for 30 min at room temperature. The reaction was stopped with 100 μL/well of 1 M HCL aq. and the plates read at 450 nm using a microplate reader (Synergy 2, BioTek, USA). Absorbance signals were expressed as fold change compared to the DMSO vehicle control (3 h Control; set to one). ELISA quality was assessed by calculating the Z-prime (Z′), as previously described (Zhang et al., 1999). Data are presented as mean ± SD and the differences between the control and test compounds were analysed using a Student's t-test or two-way ANOVA (multiple comparisons).

2.6. Deacetylase activity assay

Deacetylase activity assays were carried out as previously described (Engel et al., 2015). Briefly, parasite cell extracts were prepared from trophozoite-stage *P. falciparum* 3D7 infected erythrocytes following lysis of infected erythrocytes with 0.15% saponin (in PBS) and washing three times with PBS. The parasites were resuspended in ice-cold PBS and lysed by repeated freeze/thaw cycles. After determining the total protein concentration by Bradford assay (Protein Assay Kit II, BioRad, #5000002, USA), 0.6 mg/mL extract were dispensed into wells of a 96-well plate. Extracts were incubated with 1 μM vorinostat, panobinostat, trichostatin A (TSA), romidepsin, entinostat or tubastatin A. Ac-RGK(Ac)-AMC fluorogenic peptide (R&D Systems, USA) was added as substrate (20 μM diluted in HDAC assay buffer; Merck Millipore, Germany) and the samples incubated at 37 °C for 1 h. Activator solution (Upstate Biotechnology, USA; Merck Millipore, Germany) was added, and samples incubated for a further 10 min at RT before reading the plate on a microplate reader (Synergy 2, BioTek, USA; excitation: 360 nm, emission: 460 nm). HeLa nuclear extract (267 μg/mL) incubated with or without 1 μM trichostatin A served as an assay control as per manufacturer's instructions (Histone deacetylase assay, Merck Millipore, Germany). Two independent assays were carried out in duplicate and results were expressed as mean percent inhibition (±SD).

3. Results and discussion

3.1. Dot blot and ELISA assays to assess *P. falciparum* protein acetylation

Inhibitors of HDACs are potential new drug leads for malaria, however the lack of recombinant *P. falciparum* HDAC enzymes and tools to study inhibitor action has made mechanism of action studies and differential profiling of compounds challenging. The investigation of histone or non-histone protein acetylation changes is a useful marker of
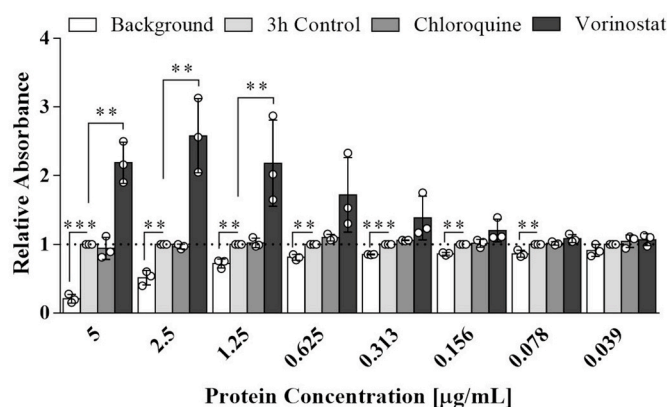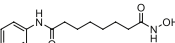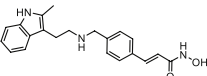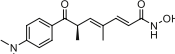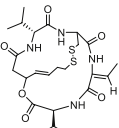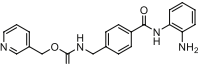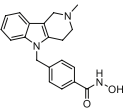

Fig. 2. Effect of different *P. falciparum* protein lysate coating concentrations on ELISA detection of histone H4 acetylation. Trophozoite-stage *P. falciparum* 3D7 infected erythrocytes treated for 3 h with 5x IC$_{50}$ chloroquine, the positive HDAC inhibitor control vorinostat or DMSO vehicle control (3 h Control, 0.125% DMSO). Protein lysates were prepared from saponin-lysed parasite pellets and 100 μL added to ELISA plate wells at 5 μg/mL/well with serial dilutions down to 39 ng/mL/well. Acetylation signal was detected with anti-(tetra)-acetyl histone H4 primary antibody (1:4000 diluted in 5% BSA in PBS) and goat anti-rabbit IgG (H/L): horseradish peroxidase (HRP) conjugate secondary antibody (1:2000 in PBS). Absorbance signals were read at 450 nm (absolute signal) and normalised (relative signal) to the untreated control (3 h Control) and expressed as fold change (3 h Control taken as 1.0; dotted line). The mean relative absorbance (±SD) for three independent biological samples are shown. *P* values * <0.05, ** <0.01, *** <0.001; multiple student's t-tests.

HDAC inhibitor action in *P. falciparum* parasites and a potential means of discerning differences in compound action that may guide downstream studies. However, this approach is currently limited to low throughput Western blot assays (e.g. (Engel et al., 2015)). In this study, we investigated two alternative approaches (dot blot and ELISA) aimed at increasing assay throughput. Both methods were established using untreated vehicle controls, chloroquine as a non-HDAC inhibitor control and vorinostat as a positive antiplasmodial HDAC inhibitor control (Engel et al., 2015) (Fig. 1, Supplementary Information **S1**). The antibody chosen for assay establishment was anti-(tetra)-acetyl histone H4 which detects AcH4 Lys5, AcH4 Lys8, AcH4 Lys12 and AcH4 Lys16. This antibody was selected because it has previously been shown to detect changes in *P. falciparum* histone lysine acetylation following vorinostat treatment using the Western blot method (Engel et al., 2015; Chua et al., 2017).

Data generated from both the dot blot and ELISA demonstrated that basal tetra-acetyl histone H4 acetylation (3 h Control) can be detected in *P. falciparum* 3D7 protein lysates using 20, 10, 5 and 2 μg/mL of protein per well. However, using 2 μg/mL protein did not achieve a significantly higher signal compared to the background noise for either assay (Fig. 1C and E, respectively). As expected (and as shown in Western blot data from this (Fig. 1A, S1) and previous studies (Engel et al., 2015; Chua et al., 2017; Mackwitz et al., 2019)), data obtained with dot blot and ELISA demonstrated no histone H4 acetylation change when the negative antimalarial control chloroquine was used (Fig. 1D and F, respectively). In contrast and also expected, the positive HDAC inhibitor control, vorinostat, was shown to increase (tetra)-acetyl histone H4 acetylation in both assays and at all protein concentrations (Fig. 1D and F, respectively). However, as a result of high assay variability, vorinostat-induced acetylation changes were not statistically significantly different to the untreated control in the dot blot assay (Fig. 1D, S1). In comparison, the vorinostat-induced acetylation changes demonstrated using the ELISA assay were significant for all protein concentrations examined (Fig. 1F, **S1**; *p*-values: 0.00095–0.0394).

As relative absorbance values in ELISA were highest when 2 μg/mL protein from vorinostat treated parasites were used (Fig. 1F), additional

Table 1

In vitro activity and human HDAC isoform selectivity of HDAC inhibitors.

Compound	Structure	Human HDAC specificity	MW (g/mol)	logP[a]	Human cell IC$_{50}$ (nM)[b]	Pf3D7 IC$_{50}$ (nM)[c]	SI[d]
Vorinostat[f]		Class I, IIa, IIb, IV	264.32	1.9	5,500	120	46
Panobinostat[g]		Class I, IIa, IIb, IV	349.43	3.0	70	10	7
Trichostatin A[h]		Class I, IIa, IIb	302.37	2.7	200	11	18
Romidepsin[i]		HDAC1, HDAC2	540.70	2.2	1	90	<1
Entinostat[j]		HDAC1, HDAC3	376.41	2.0	>20,000	8,300	>2
Tubastatin A[k]		HDAC6	335.41	2.3	2,400	150[e]	16

[a] logP derived from pubchem.ncbi.nlm.nih.gov; [b] Mammalian cell toxicity was tested against neonatal foreskin fibroblast cells (NFF) for vorinostat (Engel et al., 2015), panobinostat (Engel et al., 2015), trichostatin A (Moradei et al., 2005) and romidepsin (Engel et al., 2015), against breast fibroblasts (HS578BST) for entinostat (Ungerstedt et al., 2005) and against embryonic kidney cells (HEK293) for tubastatin A (Goracci et al., 2016); [c] IC$_{50}$s confirmed in this study (n = 1 assays; data not shown); [d] Selectivity Index: human cell IC$_{50}$/PfIC$_{50}$; [e] First report of Pf3D7 IC$_{50}$ (n = 3 assays; this study); [f] (Richon et al., 1998; Engel et al., 2015); [g] (Scuto et al., 2008; Engel et al., 2015); [h] (Vigushin et al., 2001; Andrews et al., 2008); [i] (Furumai et al., 2002; Engel et al., 2015); [j] (Rosato et al., 2003; Tatamiya et al., 2004; Andrews et al., 2008); [k] (Butler et al., 2010).

experiments were undertaken to optimise protein coating to ELISA plate wells (Fig. 2, S1; 0.039–5 μg/mL). Data from these experiments highlighted the consistency of the ELISA assay (e.g. compare 5 μg/mL samples; Figs. 1F and 2) and demonstrated that the highest ratio of acetylation signal for vorinostat when compared to untreated controls was seen using 2.5 μg/mL protein (Fig. 2; *p*-value: 0.007). Importantly, these conditions also maintained an acceptable signal to background ratio (Fig. 2; *p*-value: 0.0013; Z' = 0.719 (±0.09), calculated for three independent assays). Based on these data, the ELISA method was selected for further studies using a panel of HDAC inhibitors with demonstrated antiplasmodial activity.

3.2. Inhibition of P. falciparum deacetylase activity by HDAC inhibitors

The ability of a panel of HDAC inhibitors to inhibit *P. falciparum* deacetylase activity was first assessed using protein lysates from trophozoite-stage parasites. Compounds examined were: the FDA approved drugs vorinostat and panobinostat (both selective for class I, IIa, IIb and IV human HDACs) and romidepsin (human HDAC1 and HDAC2 selectivity) (Grant et al., 2007; Campas-Moya 2009; Garnock-Jones 2015); the human isoform selective HDAC inhibitors entinostat (human HDAC1 and HDAC3 selectivity), tubastatin A (human HDAC6 selectivity) (Tatamiya et al., 2004; Butler et al., 2010) and the pan-selective HDAC inhibitor trichostatin A (class I, IIa and IIb human HDAC selectivity) (Vigushin et al., 2001) (Table 1). With the exception of tubastatin A, the HDAC inhibitors investigated have been previously tested for *in vitro* growth inhibition against *P. falciparum* 3D7 and are active in the nanomolar to micromolar range (Andrews et al., 2008; Engel et al., 2015) (Table 1). The activity of tubastatin A at 1 μM has been previously reported (Vanheer et al., 2020); in this study we determined that tubastatin A has an *in vitro P. falciparum* 3D7 IC$_{50}$ of 150 nM (±30 nM) (Table 1).

When tested for the ability to inhibit deacetylase activity in *P. falciparum* 3D7 protein lysates, all compounds, except entinostat, caused at least 75% inhibition at 1 μM (Fig. 3). These data are consistent with previously published data for vorinostat, panobinostat, romidepsin
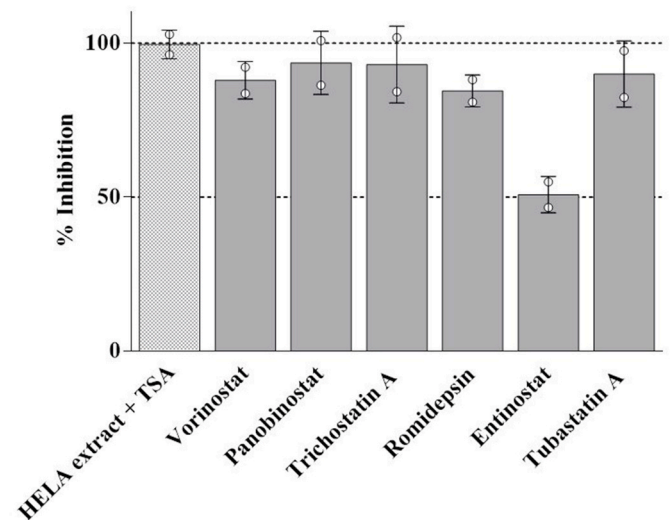

Fig. 3. Inhibition of deacetylase activity in *P. falciparum* 3D7 protein lysates. The HDAC inhibitors vorinostat, panobinostat, trichostatin A, romidepsin, entinostat and tubastatin A were assessed for deacetylase activity inhibition at 1 μM using whole cell extracts prepared from trophozoite-stage *P. falciparum* 3D7 parasites. HeLa extract, with and without 1 μM trichostatin A (TSA), was used as an assay control. The Ac-RGK(Ac)-AMC fluorogenic peptide was used as substrate and the mean percent inhibition (±SD) for two independent assays, each in duplicate, is shown.

and trichostatin A (Engel et al., 2015) and is reported here for the first time for entinostat and tubastatin A. While 1 μM entinostat resulted in only ~50% inhibition of deacetylase activity, it should be noted that entinostat was the least potent of the compounds in terms of activity against *P. falciparum* 3D7 (IC$_{50}$ 8300 nM; Table 1) which may explain the decreased deacetylase activity observed. As expected, the deacetylase activity of the HeLa extract was almost completely (99.5%) inhibited by the control HDAC inhibitor trichostatin A at 1 μM (Fig. 3).
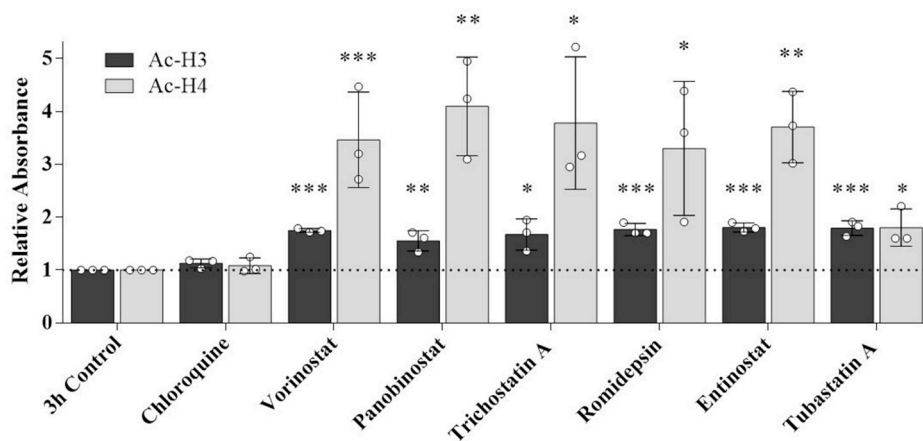
Fig. 4. Effect of HDAC inhibitor treatment on *P. falciparum* histone H3 and H4 acetylation using ELISA. Protein lysates were prepared from trophozoite-stage *P. falciparum* 3D7 infected erythrocytes treated for 3 h with 5x IC$_{50}$ (Table 1) of HDAC inhibitors vorinostat, panobinostat, trichostatin A, romidepsin, entinostat or tubastatin A. Controls included vehicle only (3 h Control, 0.5% DMSO) and the non-HDAC inhibitor control chloroquine. ELISA was carried out using 100 μL of 2.5 μg/mL protein/well. H3 and H4 acetylation were detected using anti-acetyl histone H3 primary antibody (1:2000 diluted in 5% BSA in PBS) or (tetra)-acetyl histone H4 (1:4000 diluted in 5% BSA in PBS) and goat anti-rabbit IgG (H/L): horseradish peroxidase (HRP) conjugate secondary antibody (1:2000 in PBS). Absorbance signals were read at 450 nm (absolute signal), normalised (relative signal) to the untreated control (3 h Control) and expressed as fold change (3 h Control taken as 1.0; dotted line). The mean relative absorbances for three independent biological samples (±SD) are shown. *P* values * <0.05, ** <0.01, *** <0.001; multiple student's t-tests.
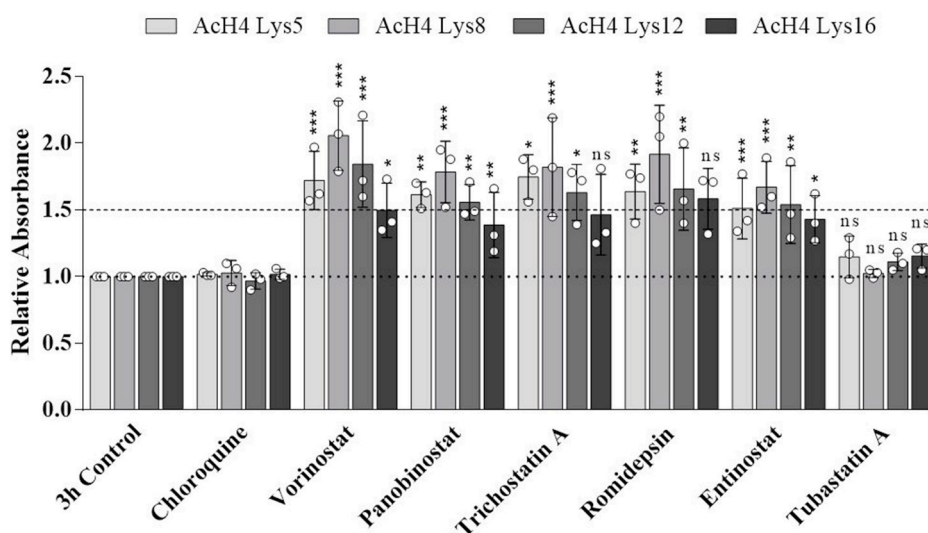

Fig. 5. Effect of HDAC inhibitor treatment on *P. falciparum* histone H4 acetylation using ELISA and different H4 acetyl-lysine antibodies. ELISA analysis of protein lysates prepared from trophozoite-stage *P. falciparum* 3D7 infected erythrocytes treated for 3 h with 5x IC$_{50}$ of HDAC inhibitors HDAC inhibitors vorinostat, panobinostat, trichostatin A, romidepsin, entinostat or tubastatin A. Controls included a DMSO vehicle control (3 h Control, 0.5% DMSO) and the non-HDAC inhibitor control chloroquine. ELISAs were carried out in 96 well plates using *P. falciparum* 3D7 protein samples at a concentration of 2.5 μg/mL (diluted in PBS), primary antibodies anti-acetyl histone H4 Lysine 5 (**AcH4 Lys5**), -Lysine 8 (**AcH4 Lys8**), -Lysine 12 (**AcH4 Lys12**) (1:2000 diluted in 5% BSA in PBS), anti-acetyl histone H4 Lysine 16 (**AcH4 Lys16**; 1:1000 diluted in 5% BSA in PBS) and goat anti-rabbit IgG (H/L):horseradish peroxidase (HRP) conjugate secondary antibody (1:2000 in PBS). Absorbance signals were read at 450 nm (absolute signal) and normalised (relative signal) to the untreated control (3 h Control) and expressed as fold change (3 h Control taken as 1.0; dotted line). The mean relative absorbance for three independent biological repeats (±SD) is shown. Dashed line indicated 1.5-fold change in relative absorbance. *P* values * <0.05, ** <0.01, *** <0.001; two way ANOVA (multiple comparisons).

3.3. Assessment of P. falciparum H3 and H4 acetylation changes following treatment with different HDAC inhibitors

ELISA was used to examine the effect of the six HDAC inhibitors (Table 1) on histone H3 and H4 acetylation in *P. falciparum* 3D7 parasites (Fig. 4, S1). Controls included a DMSO vehicle control (3 h Control) and the non-HDAC inhibitor control chloroquine. The acetylation signals detected using anti-acetyl histone H3 and anti-(tetra)-acetyl histone H4 antibodies were significantly increased for all HDAC inhibitors compared to the untreated control (Fig. 4, *p*-value: 0.035 - < 0.0001). All compounds showed ~1.8-fold increased acetylation signal using the anti-acetyl histone H3 antibody. In contrast, tubastatin A, the only HDAC inhibitor tested with selectivity for human HDAC6 (Butler et al.,

2010), showed a lower (~1.8-fold) increase in histone H4 acetylation signal compared to a mean ~3-fold, or higher, increase for the other five compounds (Fig. 4). A more detailed analysis of the N-terminal lysine acetylation profile of *P. falciparum* histone H4 was therefore carried out using antibodies recognising the individual N-terminal H4 lysines (Fig. 5, S1). The inhibitors vorinostat, romidepsin, entinostat, panobinostat and trichostatin A all caused increased acetylation (mean ~1.4–2.0-fold; Fig. 5; *p*-values: 0.0352 < 0.0001 (with the exemption of entinostat and panobinostat against AcH4 Lys16; *p*-values: 0.11–0.059)) of each of the individual H4 acetyl lysine residues. For all these inhibitors, the highest acetylation changes were detected with the anti-AcH4 Lys8 antibody, which aligns with results from Gupta et al. who tested trichostatin A against the four histone H4 lysine residues

(Gupta et al., 2017). In contrast, tubastatin A treatment resulted in no significant acetylation change using any of the antibodies specific for the different H4 acetylated lysines (Fig. 5; $p > 0.05$). Thus, it may be that for tubastatin A there is lower overall acetylation of individual *P. falciparum* H4 lysines and a slight additive hyperacetylation effect is seen when the anti-(tetra)-acetyl histone H4 antibody is used. It should also be noted that the anti-(tetra)-acetyl histone H4 antibody has been reported to cross-react with H2B/H2Bv (~13–14 kDa) and H2A.Z (~16 kDa) (Miao et al., 2006), so it is also possible that the signal observed is due to acetylation of another histone variant. These data do suggest, however, that tubastatin A, the only human HDAC6-selective compound examined, causes a different effect to the other HDAC inhibitors tested. While this will need to be further examined, including using additional antibodies to other histone variants and by determining if this effect is translated to other HDAC6-selective compounds, these data are encouraging and indicate that the activity of different HDAC inhibitors against *P. falciparum* may be discernible using an ELISA profiling strategy.

4. Conclusion

P. falciparum HDACs are under investigation as possible new drug targets for malaria. While potent and selective HDAC inhibitors have been identified, there are a number of limitations that prevent triaging of compounds for further study including a lack of robust assays to assess differential phenotypic effects. Here we developed a new ELISA method to investigate changes in *P. falciparum* histone lysine acetylation and used this assay to profile a panel of six anti-cancer HDAC inhibitors. Data revealed a different acetylation profile for tubastatin A, the only human HDAC6-selective compound examined, paving the way for further studies to elucidate the activity of this compound and other HDAC6-selective inhibitors. In summary, the ELISA developed in this study is a useful new tool that will aid in the investigation of HDAC inhibitors as drug leads for malaria.

Declarations of competing interest

None.

Acknowledgements

Appendix A. Supplementary data

Supplementary data related to this article can be found at https ://doi.org/10.1016/j.ijpddr.2020.10.010.

References

Agbor-Enoh, S., Seudieu, C., Davidson, E., Dritschilo, A., Jung, M., 2009. Novel inhibitor of *Plasmodium* histone deacetylase that cures *P. berghei*-infected mice. Antimicrob. Agents Chemother. 53, 1727–1734.

Andrews, K.T., Gupta, A.P., Tran, T.N., Fairlie, D.P., Gobert, G.N., Bozdech, Z., 2012a. Comparative gene expression profiling of *P. falciparum* malaria parasites exposed to three different histone deacetylase inhibitors. PLoS One 7, e31847.

Andrews, K.T., Haque, A., Jones, M.K., 2012b. HDAC inhibitors in parasitic diseases. Immunol. Cell Biol. 90, 66–77.

Andrews, K.T., Tran, T.N., Fairlie, D.P., 2012c. Towards histone deacetylase inhibitors as new antimalarial drugs. Curr. Pharmaceut. Des. 18, 3467–3479.

Andrews, K.T., Tran, T.N., Lucke, A.J., Kahnberg, P., Le, G.T., Boyle, G.M., Gardiner, D. L., Skinner-Adams, T.S., Fairlie, D.P., 2008. Potent antimalarial activity of histone deacetylase inhibitor analogues. Antimicrob. Agents Chemother. 52, 1454–1461.

Andrews, K.T., Tran, T.N., Wheatley, N.C., Fairlie, D.P., 2009. Targeting histone deacetylase inhibitors for anti-malarial therapy. Curr. Top. Med. Chem. 9, 292–308.

Aurrecoechea, C., Brestelli, J., Brunk, B.P., Dommer, J., Fischer, S., Gajria, B., Gao, X., Gingle, A., Grant, G., Harb, O.S., Heiges, M., Innamorato, F., Iodice, J., Kissinger, J. C., Kraemer, E., Li, W., Miller, J.A., Nayak, V., Pennington, C., Pinney, D.F., Roos, D. S., Ross, C., Stoeckert Jr., C.J., Treatman, C., Wang, H., 2009. PlasmoDB: a functional genomic database for malaria parasites. Nucleic Acids Res. 37, D539–D543.

Butler, K.V., Kalin, J., Brochier, C., Vistoli, G., Langley, B., Kozikowski, A.P., 2010. Rational design and simple chemistry yield a superior, neuroprotective HDAC6 inhibitor, tubastatin A. J. Am. Chem. Soc. 132, 10842–10846.

Campas-Moya, C., 2009. Romidepsin for the treatment of cutaneous T-cell lymphoma. Drugs Today (Barc). 45, 787–795.

Chenet, S.M., Akinyi Okoth, S., Huber, C.S., Chandrabose, J., Lucchi, N.W., Talundzic, E., Krishnalall, K., Ceron, N., Musset, L., Macedo de Oliveira, A., Venkatesan, M., Rahman, R., Barnwell, J.W., Udhayakumar, V., 2016. Independent emergence of the *Plasmodium falciparum* kelch propeller domain mutant Allele C580Y in Guyana. J. Infect. Dis. 213, 1472–1475.

Chua, M.J., Arnold, M.S., Xu, W., Lancelot, J., Lamotte, S., Spath, G.F., Prina, E., Pierce, R.J., Fairlie, D.P., Skinner-Adams, T.S., Andrews, K.T., 2017. Effect of clinically approved HDAC inhibitors on *Plasmodium, Leishmania* and *Schistosoma* parasite growth. Int J Parasitol Drugs Drug Resist 7, 42–50.

Coetzee, N., von Gruning, H., Opperman, D., van der Watt, M., Reader, J., Birkholtz, L. M., 2020. Epigenetic inhibitors target multiple stages of *Plasmodium falciparum* parasites. Sci. Rep. 10, 2355.

Coleman, B.I., Skillman, K.M., Jiang, R.H.Y., Childs, L.M., Altenhofen, L.M., Ganter, M., Leung, Y., Goldowitz, I., Kafsack, B.F.C., Marti, M., Llinas, M., Buckee, C.O., Duraisingh, M.T., 2014. A *Plasmodium falciparum* histone deacetylase regulates antigenic variation and gametocyte conversion. Cell Host Microbe 16, 177–186.

Darkin-Rattray, S.J., Gurnett, A.M., Myers, R.W., Dulski, P.M., Crumley, T.M., Allocco, J. J., Cannova, C., Meinke, P.T., Colletti, S.L., Bednarek, M.A., Singh, S.B., Goetz, M.A., Dombrowski, A.W., Polishook, J.D., Schmatz, D.M., 1996. Apicidin: a novel antiprotozoal agent that inhibits parasite histone deacetylase. Proc. Natl. Acad. Sci. U. S. A. 93, 13143–13147.

Duraisingh, M.T., Voss, T.S., Marty, A.J., Duffy, M.F., Good, R.T., Thompson, J.K., Freitas-Junior, L.H., Scherf, A., Crabb, B.S., Cowman, A.F., 2005. Heterochromatin silencing and locus repositioning linked to regulation of virulence genes in *Plasmodium falciparum*. Cell 121, 13–24.

Engel, J.A., Jones, A.J., Avery, V.M., Sumanadasa, S.D., Ng, S.S., Fairlie, D.P., Adams, T. S., Andrews, K.T., 2015. Profiling the anti-protozoal activity of anti-cancer HDAC inhibitors against *Plasmodium* and *Trypanosoma* parasites. Int J Parasitol Drugs Drug Resist 5, 117–126.

Fioravanti, R., Mautone, N., Rovere, A., Rotili, D., Mai, A., 2020. Targeting histone acetylation/deacetylation in parasites: an update (2017-2020). Curr. Opin. Chem. Biol. 57, 65–74.

Freitas-Junior, L.H., Hernandez-Rivas, R., Ralph, S.A., Montiel-Condado, D., Ruvalcaba-Salazar, O.K., Rojas-Meza, A.P., Mancio-Silva, L., Leal-Silvestre, R.J., Gontijo, A.M., Shorte, S., Scherf, A., 2005. Telomeric heterochromatin propagation and histone acetylation control mutually exclusive expression of antigenic variation genes in malaria parasites. Cell 121, 25–36.

Furumai, R., Matsuyama, A., Kobashi, N., Lee, K.H., Nishiyama, M., Nakajima, H., Tanaka, A., Komatsu, Y., Nishino, N., Yoshida, M., Horinouchi, S., 2002. FK228 (depsipeptide) as a natural prodrug that inhibits class I histone deacetylases. Canc. Res. 62, 4916–4921.

Garnock-Jones, K.P., 2015. Panobinostat: first global approval. Drugs 75, 695–704.

Giannini, G., Battistuzzi, G., Vignola, D., 2015. Hydroxamic acid based histone deacetylase inhibitors with confirmed activity against the malaria parasite. Bioorg. Med. Chem. Lett 25, 459–461.

Goracci, L., Deschamps, N., Randazzo, G.M., Petit, C., Dos Santos Passos, C., Carrupt, P. A., Simoes-Pires, C., Nurisso, A., 2016. A rational approach for the identification of non-hydroxamate HDAC6-selective inhibitors. Sci. Rep. 6, 29086.

Grant, S., Easley, C., Kirkpatrick, P., 2007. Vorinostat. Nat. Rev. Drug Discov. 6, 21–22.

Gupta, A.P., Zhu, L., Tripathi, J., Kucharski, M., Patra, A., Bozdech, Z., 2017. Histone 4 lysine 8 acetylation regulates proliferation and host-pathogen interaction in *Plasmodium falciparum*. Epigenet. Chromatin 10, 40.

Hailu, G.S., Robaa, D., Forgione, M., Sippl, W., Rotili, D., Mai, A., 2017. Lysine deacetylase inhibitors in parasites: past, present, and future perspectives. J. Med. Chem. 60, 4780–4804.

Hollin, T., Gupta, M., Lenz, T., Le Roch, K.G., 2020. Dynamic chromatin structure and epigenetics control the fate of malaria parasites. Trends Genet. S0168–9525 (20), 30239-0.

Kanyal, A., Rawat, M., Gurung, P., Choubey, D., Anamika, K., Karmodiya, K., 2017. Genome-wide survey and phylogenetic analysis of histone acetyltransferases and histone deacetylases of *Plasmodium falciparum*. FEBS J. 285, 1767–1782.

Khan, O., La Thangue, N.B., 2012. HDAC inhibitors in cancer biology: emerging mechanisms and clinical applications. Immunol. Cell Biol. 90, 85–94.

Lambros, C., Vanderberg, J.P., 1979. Synchronization of *Plasmodium falciparum* erythrocytic stages in culture. J. Parasitol. 65, 418–420.

Lu, F., Culleton, R., Zhang, M., Ramaprasad, A., von Seidlein, L., Zhou, H., Zhu, G., Tang, J., Liu, Y., Wang, W., Cao, Y., Xu, S., Gu, Y., Li, J., Zhang, C., Gao, Q., Menard, D., Pain, A., Yang, H., Zhang, Q., Cao, J., 2017. Emergence of indigenous artemisinin-resistant *Plasmodium falciparum* in Africa. N. Engl. J. Med. 376, 991–993.

Mackwitz, M.K.W., Hesping, E., Antonova-Koch, Y., Diedrich, D., Woldearegai, T.G., Skinner-Adams, T., Clarke, M., Scholer, A., Limbach, L., Kurz, T., Winzeler, E.A., Held, J., Andrews, K.T., Hansen, F.K., 2019. Structure-activity and structure-toxicity relationships of peptoid-based histone deacetylase inhibitors with dual-stage antiplasmodial activity. ChemMedChem 14, 912–926.

Melesina, J., Robaa, D., Pierce, R.J., Romier, C., Sippl, W., 2015. Homology modeling of parasite histone deacetylases to guide the structure-based design of selective inhibitors. J. Mol. Graph. Model. 62, 342–361.

Merrick, C.J., Duraisingh, M.T., 2007. *Plasmodium falciparum* Sir2: an unusual sirtuin with dual histone deacetylase and ADP-ribosyltransferase activity. Eukaryot. Cell 6, 2081–2091.

Miao, J., Fan, Q., Cui, L., Li, J., Li, J., Cui, L., 2006. The malaria parasite *Plasmodium falciparum* histones: organization, expression, and acetylation. Gene 369, 53–65.

Moradei, O., Maroun, C.R., Paquin, I., Vaisburg, A., 2005. Histone deacetylase inhibitors: latest developments, trends and prospects. Curr Med Chem Anticancer Agents 5, 529–560.

Ontoria, J.M., Paonessa, G., Ponzi, S., Ferrigno, F., Nizi, E., Biancofiore, I., Malancona, S., Graziani, R., Roberts, D., Willis, P., Bresciani, A., Gennari, N., Cecchetti, O., Monteagudo, E., Orsale, M.V., Veneziano, M., Di Marco, A., Cellucci, A., Laufer, R., Altamura, S., Summa, V., Harper, S., 2016. Discovery of a selective series of inhibitors of *Plasmodium falciparum* HDACs. ACS Med. Chem. Lett. 7, 454–459.

Prince, H.M., Dickinson, M., Khot, A., 2013. Romidepsin for cutaneous T-cell lymphoma. Future Oncol. 9, 1819–1827.

Rasmussen, C., Nyunt, M.M., Ringwald, P., 2017. Artemisinin-Resistant *Plasmodium falciparum* in Africa. N. Engl. J. Med. 377, 305–306.

Richon, V.M., Emiliani, S., Verdin, E., Webb, Y., Breslow, R., Rifkind, R.A., Marks, P.A., 1998. A class of hybrid polar inducers of transformed cell differentiation inhibits histone deacetylases. Proc. Natl. Acad. Sci. U. S. A. 95, 3003–3007.

Rosato, R.R., Almenara, J.A., Grant, S., 2003. The histone deacetylase inhibitor MS-275 promotes differentiation or apoptosis in human leukemia cells through a process regulated by generation of reactive oxygen species and induction of p21CIP1/WAF1 1. Canc. Res. 63, 3637–3645.

Scuto, A., Kirschbaum, M., Kowolik, C., Kretzner, L., Juhasz, A., Atadja, P., Pullarkat, V., Bhatia, R., Forman, S., Yen, Y., Jove, R., 2008. The novel histone deacetylase inhibitor, LBH589, induces expression of DNA damage response genes and apoptosis in Ph- acute lymphoblastic leukemia cells. Blood 111, 5093–5100.

Shahbazian, M.D., Grunstein, M., 2007. Functions of site-specific histone acetylation and deacetylation. Annu. Rev. Biochem. 76, 75–100.

Sumanadasa, S.D., Goodman, C.D., Lucke, A.J., Skinner-Adams, T., Sahama, I., Haque, A., Do, T.A., McFadden, G.I., Fairlie, D.P., Andrews, K.T., 2012. Antimalarial activity of the anticancer histone deacetylase inhibitor SB939. Antimicrob. Agents Chemother. 56, 3849–3856.

Tatamiya, T., Saito, A., Sugawara, T., Nakanishi, O., 2004. Isozyme-selective activity of the HDAC inhibitor MS-275. Canc. Res. 64, 567-567.

Thompson, C.A., 2014. Belinostat approved for use in treating rare lymphoma. Am. J. Health Syst. Pharm. 71, 1328.

Tonkin, C.J., Carret, C.K., Duraisingh, M.T., Voss, T.S., Ralph, S.A., Hommel, M., Duffy, M.F., Silva, L.M., Scherf, A., Ivens, A., Speed, T.P., Beeson, J.G., Cowman, A.F., 2009. Sir2 paralogues cooperate to regulate virulence genes and antigenic variation in *Plasmodium falciparum*. PLoS Biol. 7, e84.

Trager, W., Jensen, J.B., 2005. Human malaria parasites in continuous culture. 1976. J. Parasitol. 91, 484–486.

Ungerstedt, J.S., Sowa, Y., Xu, W.S., Shao, Y., Dokmanovic, M., Perez, G., Ngo, L., Holmgren, A., Jiang, X., Marks, P.A., 2005. Role of thioredoxin in the response of normal and transformed cells to histone deacetylase inhibitors. Proc. Natl. Acad. Sci. U. S. A. 102, 673–678.

Uwimana, A., Legrand, E., Stokes, B.H., Ndikumana, J.M., Warsame, M., Umulisa, N., Ngamije, D., Munyaneza, T., Mazarati, J.B., Munguti, K., Campagne, P., Criscuolo, A., Ariey, F., Murindahabi, M., Ringwald, P., Fidock, D.A., Mbituyumuremyi, A., Menard, D., 2020. Emergence and clonal expansion of *in vitro* artemisinin-resistant *Plasmodium falciparum* kelch13 R561H mutant parasites in Rwanda. Nat. Med. 26, 1602–1608.

van der Pluijm, R.W., Imwong, M., Chau, N.H., Hoa, N.T., Thuy-Nhien, N.T., Thanh, N.V., Jittamala, P., Hanboonkunupakarn, B., Chutasmit, K., Saelow, C., Runjarern, R., Kaewmok, W., Tripura, R., Peto, T.J., Yok, S., Suon, S., Sreng, S., Mao, S., Oun, S., Yen, S., Amaratunga, C., Lek, D., Huy, R., Dhorda, M., Chotivanich, K., Ashley, E.A., Mukaka, M., Waithira, N., Cheah, P.Y., Maude, R.J., Amato, R., Pearson, R.D., Goncalves, S., Jacob, C.G., Hamilton, W.L., Fairhurst, R.M., Tarning, J., Winterberg, M., Kwiatkowski, D.P., Pukrittayakamee, S., Hien, T.T., Day, N.P., Miotto, O., White, N.J., Dondorp, A.M., 2019. Determinants of dihydroartemisinin-piperaquine treatment failure in *Plasmodium falciparum* malaria in Cambodia, Thailand, and Vietnam: a prospective clinical, pharmacological, and genetic study. Lancet Infect. Dis. 19, 952–961.

Vanheer, L.N., Zhang, H., Lin, G., Kafsack, B.F.C., 2020. Activity of epigenetic inhibitors against *Plasmodium falciparum* asexual and sexual blood stages. Antimicrob. Agents Chemother. 64 (7) e02523-19.

Vigushin, D.M., Ali, S., Pace, P.E., Mirsaidi, N., Ito, K., Adcock, I., Coombes, R.C., 2001. Trichostatin A is a histone deacetylase inhibitor with potent antitumor activity against breast cancer in vivo. Clin. Canc. Res. 7, 971–976.

Walliker, D., Quakyi, I.A., Wellems, T.E., McCutchan, T.F., Szarfman, A., London, W.T., Corcoran, L.M., Burkot, T.R., Carter, R., 1987. Genetic analysis of the human malaria parasite *Plasmodium falciparum*. Science 236, 1661–1666.

World Health Organisation, 2019. World malaria report. https://www.who.int/publications/i/item/world-malaria-report-2019.

Zhang, J.H., Chung, T.D., Oldenburg, K.R., 1999. A simple statistical parameter for use in evaluation and validation of high throughput screening assays. J. Biomol. Screen 4, 67–73.

Zhang, M., Wang, C., Otto, T.D., Oberstaller, J., Liao, X., Adapa, S.R., Udenze, K., Bronner, I.F., Casandra, D., Mayho, M., Brown, J., Li, S., Swanson, J., Rayner, J.C., Jiang, R.H.Y., Adams, J.H., 2018. Uncovering the essential genes of the human malaria parasite *Plasmodium falciparum* by saturation mutagenesis. Science 360.